JOURNAL OF MATERIALS SCIENCE **35** (2000) 31–38

Selective laser sintering of gas atomized M2 high speed steel powder

H. J. NIU, I. T. H. CHANG
School of Metallurgy and Materials, The University of Birmingham, Edgbaston, Birmingham, B15 2TT, UK
E-mail: H.NIU@bham.ac.uk

Selective laser sintering of the gas atomized M2 high speed steel powder was performed using laser powers of 2.5–100 W, scan rates of 1–30 mm/s and scan line spacings of 0.15–0.75 mm. With increasing laser power, the sintered surface varied from open/closed pores to a fully dense structure. Large lateral pores were found in the sintered surface of samples using high scan rates. For fully dense samples, smooth surfaces could be achieved using large scan line spacing. The as-supplied and sieved M2 powder particles with size ranging from 0.04 to 400 μm and 53 to 150 μm, respectively, were found to give better laser sinterability as compared with those powder particles with finer (<38 μm) or coarser (>150 μm) sizes.

1. Introduction

Selective laser sintering (SLS) is a solid freeform fabrication technology that allows direct production of metallic parts without part-specific tooling or human intervention [1]. In this process, a computer controlled laser is scanned across the surface of a loose powder bed. This allows the sintering of the powders into the shape of the required cross section. The parts is built up layer by layer from the bottom to the top. Thus, it is an additive approach to manufacture three-dimensional parts of any geometry ranging from a simple to complex shapes.

In order to increase the sintered density and decrease the processing time, direct laser sintering is desirable [2]. This involves the melting and solidification of the powder bed directly to form a dense layer so as to build the final object. Direct laser sintering of metallic parts is a complex metallurgical process which can be influenced by several phenomena, such as Marangoni flow and Rayleigh instability that are commonly found in laser welding and liquid phase sintering applications [3–5]. The sintered density and surface roughness are strongly influenced by surface active elements, powder size and shape, and processing parameters, such as laser power, scan rate and scan line spacing. Extensive research is needed to understand the effect of these factors on the SLS process. High speed steels (HSSs) are conventional cutting tool materials with a desired combination of hot hardness, wear resistance, and toughness. A time-consuming, expensive and carefully controlled processes, including hot working, heat treatment and machining, are need to produce the finished product of HSS. Currently, extensive studies have been carried out in sintering HSSs and HSS metal matrix [6, 7].

SLS of the water atomized M3/2 powder with different particle sizes produces poor surface density with large agglomerates and inter-agglomerate pores [8]. However, SLS of the gas atomized M2 powder produces homogeneous sintered structure with a highly dense surface [8]. This is attributed to high packing density, spherical shape and low oxygen of the gas atomized M2 powder particles. This paper presents a detailed study of SLS of gas atomized M2 HSS powder. It aims to understand the effect of the particle size and the SLS processing parameters on the surface morphologies and internal microstructure of laser sintered M2 powder, and determine the optimum SLS processing parameters for the gas atomized M2 powder.

2. Experimental

The materials used in this work was gas atomized M2 HSS powder supplied by Powdrex Limited, with the chemical compositions 0.996C-6.32W-5.03Mo-3.93 Cr-1.78V-0.193Mn-0.312Si-0.30Co-0.330Ni-0.252 Cu-0.020S-0.031P (wt %). The as-supplied powder was sieved through a series of mesh size to extract powder of different particle size. The particle size distribution was analyzed using a Coulter LS230 laser particle size analyzer. The oxygen level in the powder of the different particle size was determined using LECO oxygen analyzer.

A 600 W, CW, CO_2 laser with a beam size of 0.5 mm in diameter was used to perform the SLS experiment. The laser was operated at powers ranging from 2.5 to 100 W with scan rates in the range of 1 and 30 mm/s and scan line spacings ranging from 0.15 to 0.75 mm. The loose HSS powders were first loaded inside a mild steel container protected by an argon atmosphere and they

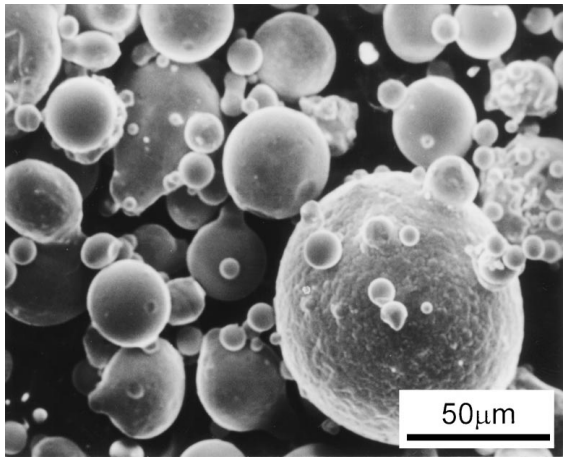

Figure 1 SEM images of HSS powders showing the shape of particles as supplied M2 HSS powder.

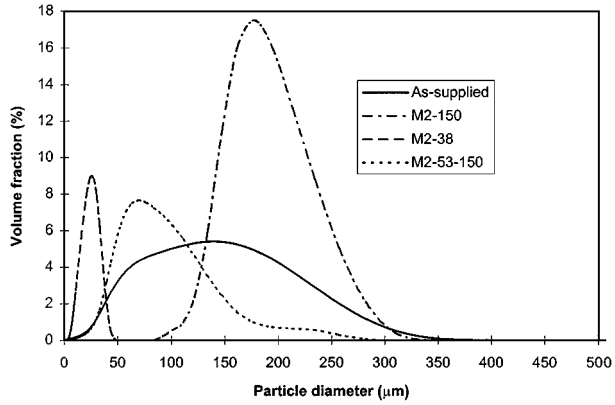

Figure 2 The distribution of the particle size of the as-supplied and sieved M2 HSS powder.

were leveled by a blade so as to obtain a flat powder surface. The thickness of the powder bed was maintained about 5 mm. The laser beam was then scanned over an area of 10×10 mm^2 on the surface of the powder bed to sinter the powder particles together.

The laser sintered samples for metallographic examination were prepared using standard techniques. Both as-sintered and polished surfaces were observed in a JEOL 5410 and 6300 scanning electron microscope (SEM) equipped with a QX2000 energy dispersive X-ray (EDX) micro analyzer for chemical composition measurement. Phase identification was performed with an X-ray diffractometer (XRD) using a Cu K_α radiation and 0.2°/min step increment.

3. Results

3.1. Powder characteristics

The as-supplied M2 powder particles had a uniform spherical morphology, as shown in Fig. 1. The apparent and top density of the powder were 4.74 and 5.15 g/cm^3, respectively. In order to study the effect of particle size, the as-supplied powder was sieved through a range of mesh size to yield the following grades:

1. above 150 μm
2. 53–150 μm
3. below 38 μm.

The particle size distribution of the as-supplied powder and sieved powders was given in Fig. 2. The mean particle diameter of the as-supplied powder was 117 μm and the volume fraction particle size below 216 μm corresponded 90%, and below 38 μm 10%.

Oxygen content for as-supplied powder, sieved fine (<38 μm) and large (>150 μm) powder were 200, 375 and 130 ppm, respectively. The oxygen level increased with decreasing the mean particle size.

3.2. Surface morphologies

3.2.1. Effect of laser power

Fig. 3 shows the surface morphologies of M2 HSS laser sintered samples using a fixed scan rate of 1.0 mm/s and a scan line spacing of 0.15 mm for various laser powers ranging from 5 W to 50 W. At a low laser power of 5 W (Fig. 3a), the sintered surface consisted of agglomerates and open pores, leading to a randomly equiaxed structure. Such structure also contained some remaining unsintered starting powder particles. At a high laser power of 10 W (Fig. 3b), the agglomerates coarsened significantly and appeared more dense. In addition, the pores around the agglomerates began to merge and appeared interconnected. At an even higher laser power of 35 W (Fig. 3c), the morphology of the agglomerates disappeared and a continuous skeleton structure was developed. This produced a fairly dense structure with closed pores. Finally, at laser powers higher than 40 W, SLS resulted in the formation of a fully dense surface (Fig. 3d) without any pores in the structure.

3.2.2. Effect of scan rate

The surface morphologies of M2 HSS laser sintered samples using a fixed scan line spacing of 0.15 mm, laser powers of 5–35 W and scan rates of 5–15 mm/s are shown in Fig. 4. As compared with Fig. 3, laser sintering at a scan rate of 5 mm/s resulted in the formation of finer surface structure, small agglomerates and reduced pore size. At a low laser power of 5 W, initial stage of agglomerate development occurred (Fig. 4a) and necking of several M2 powder particles were found. At a high laser power of 10 W, more connection between agglomerates developed and this led to an increasing agglomerate size (Fig. 4b). Although the internal density of the agglomerates (i.e. fraction of solid region) formed at 5 mm/s was lower than that at 1 mm/s, the size of inter-agglomerate pore was much smaller (Figs 3b and 4b). At an even higher laser power of 35 W, laser sintering at a scan rate to 5 mm/s resulted in the formation of the relatively smooth and almost fully dense surface (Fig. 4c). However, at the same laser power of 35 W, laser sintering at a high scan rate of 20 mm/s produced relatively large lateral pores in the surface, as shown in Fig. 4d. The experimental results show that a critical scan rate exists for the formation of the lateral pores, which increases with increasing laser power.

Fig. 5 summaries the change of porosity in the laser sintered surface with increasing scan rates and various

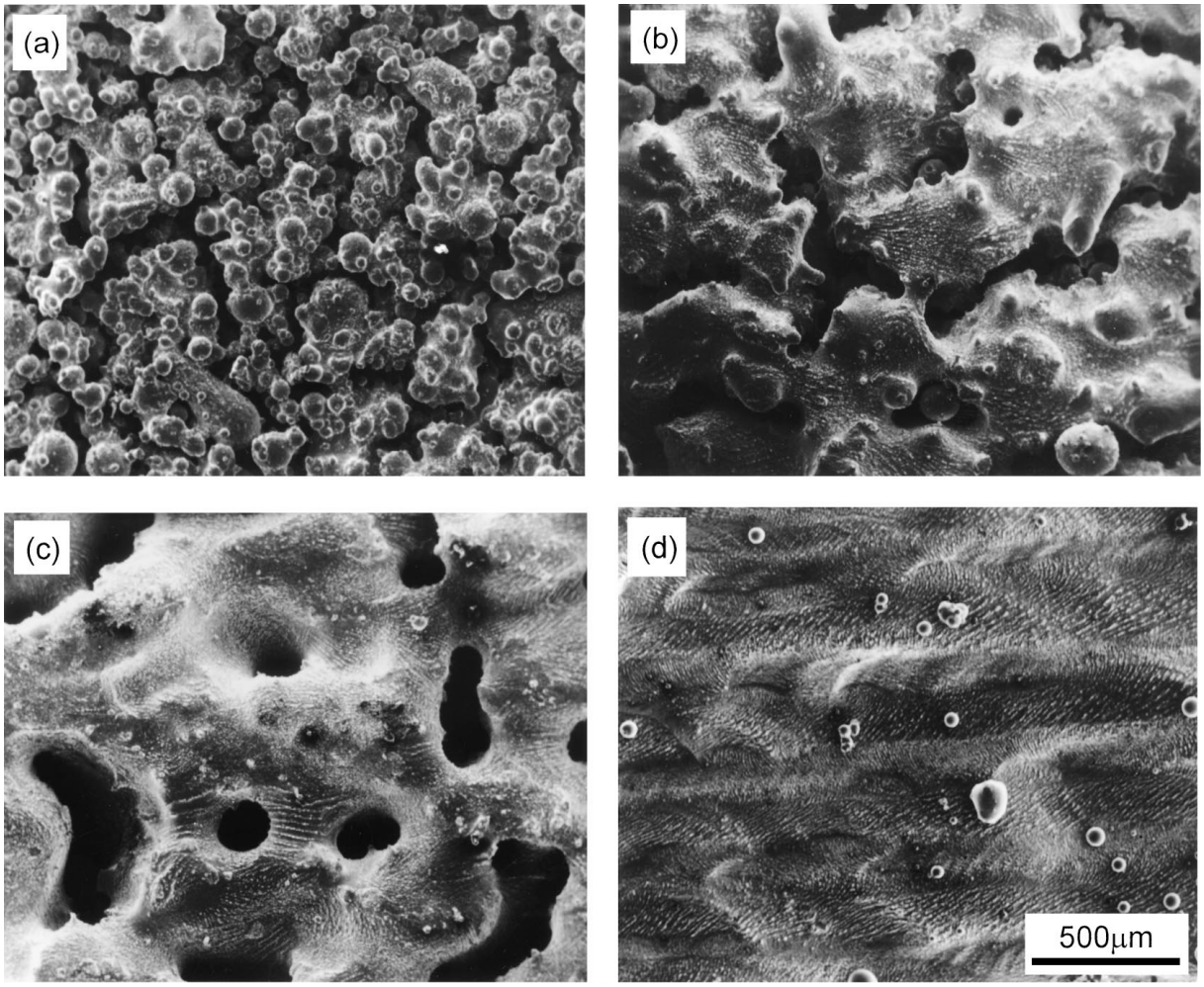

Figure 3 SEM images of laser sintered M2 surfaces using different laser powers, a scan rate of 1.0 mm/s and a scan line spacing of 0.15 mm: (a) 5 W; (b) 10 W; (c) 35 W; (d) 50 W (Scan direction ↔).

laser powers for a given scan line spacing of 0.15 mm. At laser powers below 20 W, the pores appeared open, or interconnected, and the sample density was low for all scan rates from 1 to 36 mm/s. At laser powers between 20 and 40 W, the pores were found to be large and irregular at low scan rate. However, at similar laser powers, the pores decreased and became isolated with increasing scan rates. Further increase of the scan rate produced large and lateral pores in the sintered surface. At laser powers above 40 W, the sintered surface changed from a fully dense structure to closed pore or lateral pore structure with increasing scan rate. It was worthy noting that although high laser power induced high surface density, it also tended to increase surface roughness and the inaccuracy of the part size.

3.2.3. Effect of scan line spacing

Increasing scan line spacing resulted in a decrease of incident energy density, which is defined as

$$E = \frac{P}{V \cdot H}$$

where P is the incident laser power (Watt)
V is the laser scan rate (mm/s)
H is the scan line spacing (mm)

Fig. 6 shows the effect of scan line spacing with various linear energy P/V value on the fully dense region for laser sintering at a laser power of 80 W. With increasing scan line spacing, the limit P/V value required for obtaining fully dense surface increased linearly. However, increasing scan line spacing to an appropriate value for a given P/V value can improve surface roughness. Fig. 7 shows laser sintering surface at a laser power of 50 W and a scan rate of 5 mm/s for scan line spacings of 0.55 and 0.75 mm. Increasing scan line spacing led to a significant improvement of surface roughness. However, increasing scan line spacing enhanced the formation of the lateral pores at higher laser powers, as shown in Fig. 8.

3.2.4. Effect of particle size

The surface morphologies of laser sintering samples at a laser power of 50 W, a scan rate of 5 mm/s, and a scan line spacing of 0.15 mm for various particle sizes are shown in Fig. 9. Laser sintering of the as-supplied M2 powder and the sieved M2 powder with particle sizes ranging from 53 to 150 μm led to the formation of a fully dense surface. However, for M2 powder with larger particle size (>150 μm), the incident laser power seemed to be insufficient to produce a fully dense surface (Fig. 9c). On other hand, laser sintering of the finer powder particles (<38 μm) caused large pores at

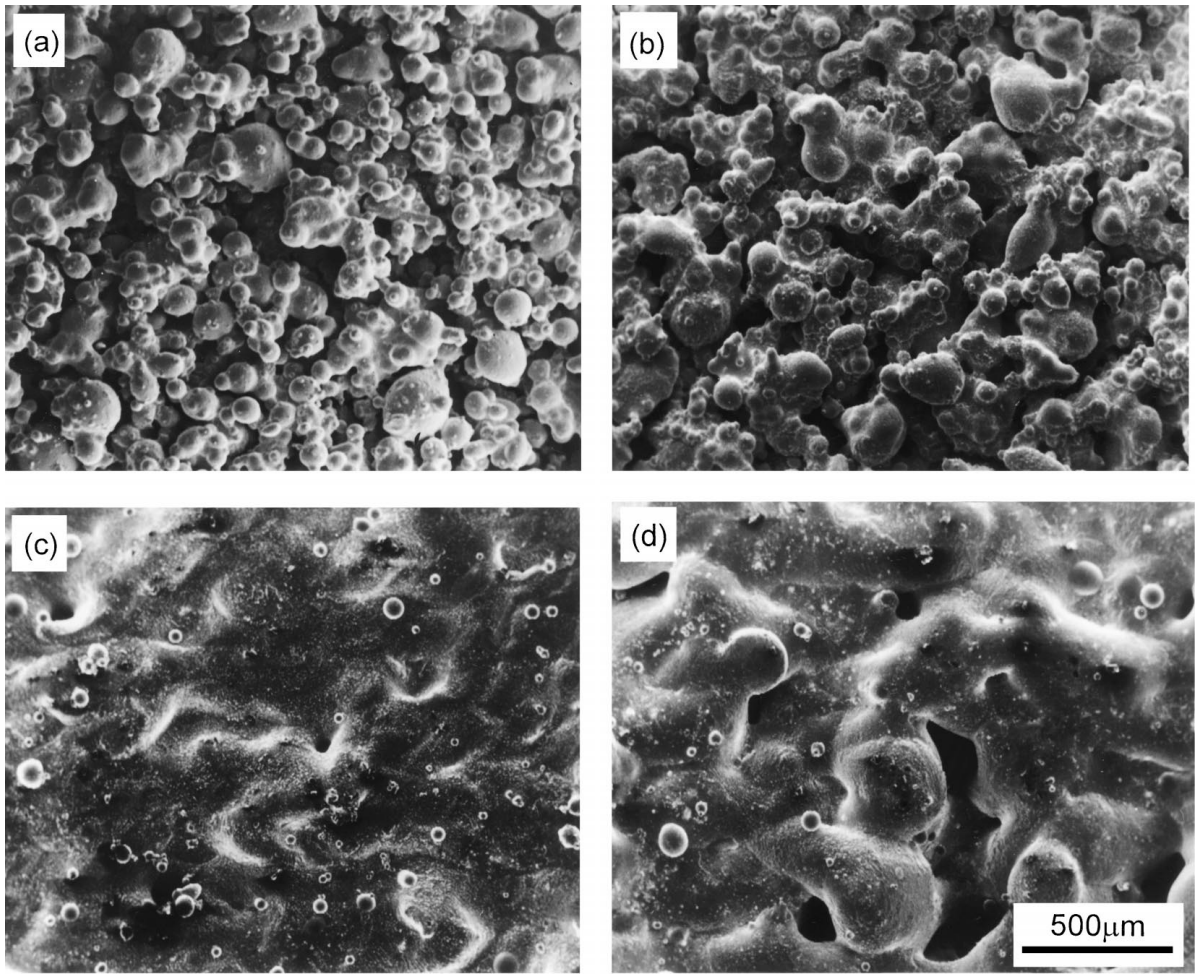

Figure 4 SEM images of laser sintered M2 surfaces using different laser powers and scan rates, and a scan line spacing of 0.15 mm: (a) 5 W, 5 mm/s; (b) 10 W, 5 mm/s; (c) 35 W, 5 mm/s; (d) 35 W, 20 mm/s (Scan direction ↔).

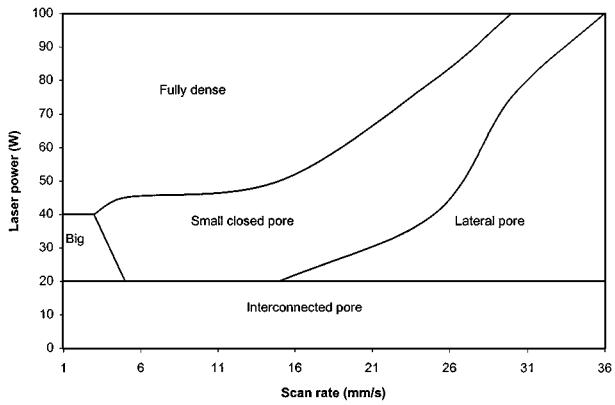

Figure 5 Variation of the porosity morphologies with scan rates for various laser powers for a given scan line spacing of 0.15 mm.

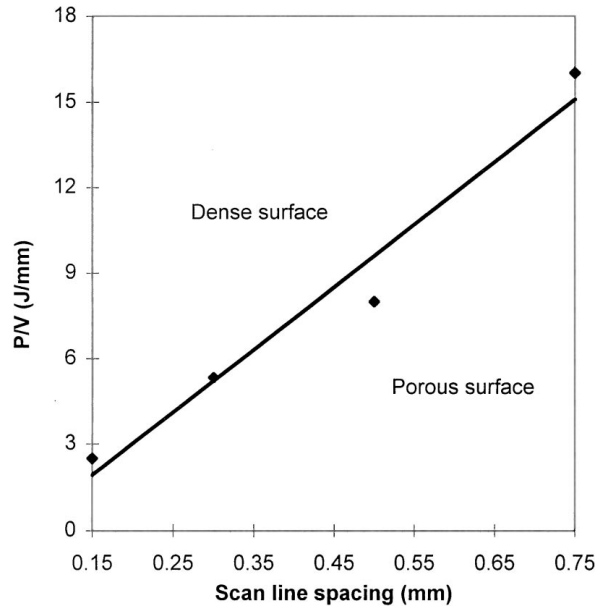

Figure 6 The effect of scan line spacings on surface density for various linear energies.

the center of the sample (Fig. 9d). SEM observation shows that the pore parallel to scan direction tended to form in the surface of laser sintering of the fine powder (<38 μm). Laser sintering of the fine powder (<38 μm) at laser powers from 5 to 50 W produced porous structures.

3.3. Microstructure of M2 steel before and after SLS

Fig. 10 shows XRD patterns of the as-supplied M2 powder and the laser sintered samples using a fixed scan rate of 1 mm/s, a scan line spacing of 0.15 mm and laser powers between 2.5 and 50 W. The as-supplied M2 powder consisted of ferrite, retained austenite, and M_4C_3 and a trace of M_6C carbides. As laser power increased, the peak of retained austenite decreased and

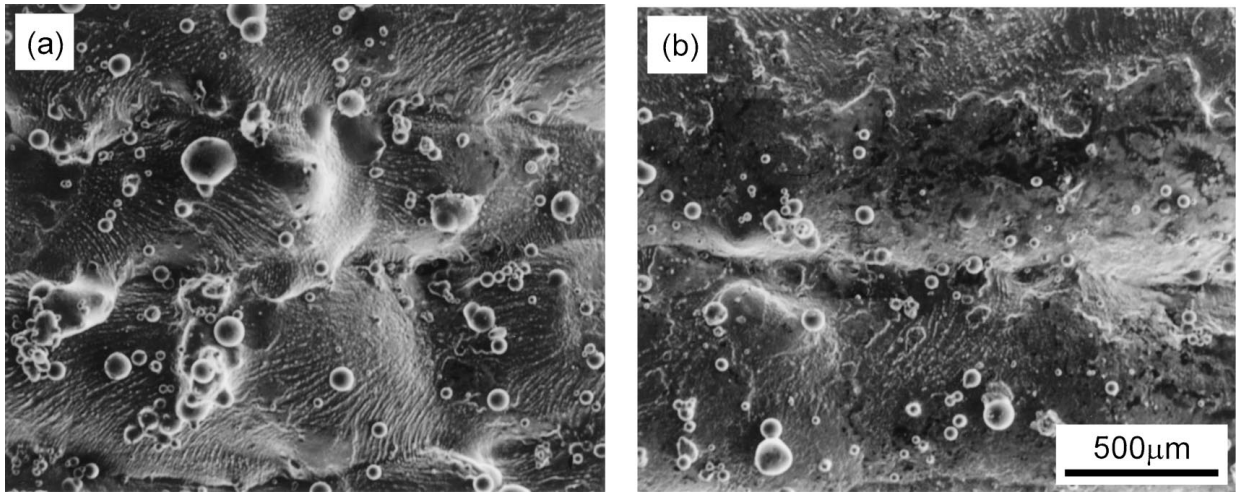

Figure 7 SEM images of laser sintered M2 surfaces using different scan line spacings, a laser power of 50 W and a scan rate of 5.0 mm/s: (a) 0.5 mm; (b) 0.75 mm (Scan direction ↔).

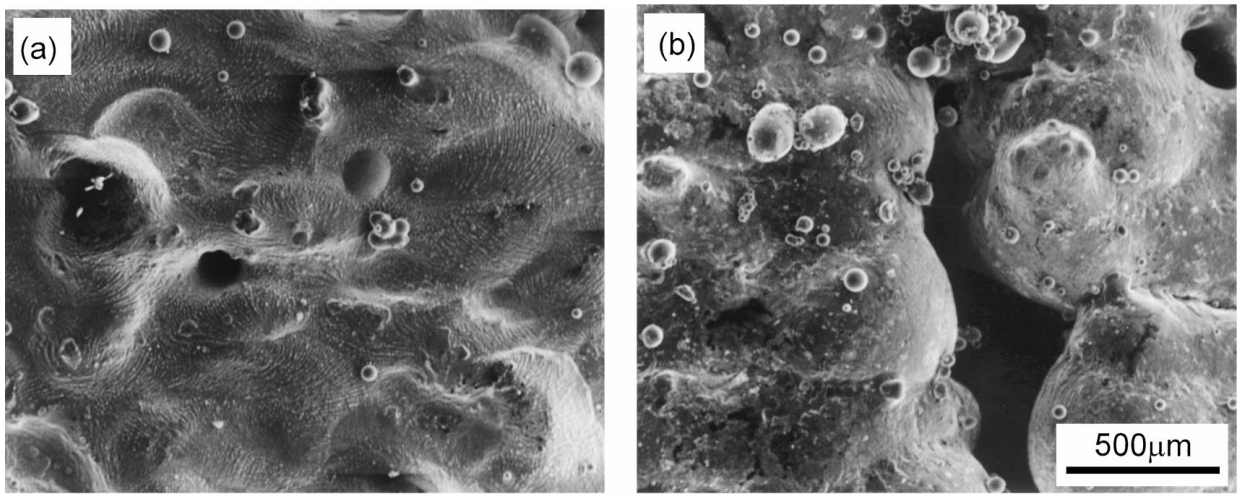

Figure 8 SEM images of laser sintered M2 surfaces using different scan line spacings, a laser power of 30 W and a scan rate of 10.0 mm/: (a) 0.15 mm; (b) 0.30 mm (Scan direction ↔).

disappeared when the laser power reached to 25 W. M_4C_3 carbide first decreased rapidly at a lower laser power of 2.5 W, and then increased significantly when a laser power was higher than 25 W. However, M_6C carbide appeared to increase with increasing laser power.

Fig. 11 shows the microstructure of the as-supplied M2 powder and the laser sintered samples using laser powers between 2.5 and 50 W, a scan rate of 1 mm/s and a scan line spacing of 0.15 mm. The microstructure of as-supplied M2 powder consisted of a ferrite matrix together with a mixture of austenite and carbides at the grain boundaries. Laser sintering at a power of 10 W resulted in dissolution of M_4C_3 carbides into the matrix and formation of more M_6C carbides at the three grain junctions, as shown in Fig. 11b. However, M_4C_3 carbides began to appear at the grain boundaries when the samples were sintered at a laser power of 25 W. As the laser power increased to 50 W, more M_6C and M_4C_3 carbides precipitated at the grain boundaries. The mean grain size of the matrix was smaller than 10 μm, and the compositions of M_4C_3 and M_6C were analyzed by EDX and listed in Table 1.

TABLE I The content of main alloying elements in M_4C_3 and M_6C carbides (at %)

Carbide	Fe	W	Mo	Cr	V
M_6C	53.041	13.377	20.672	6.738	6.171
M_4C_3	54.556	3.477	6.281	6.991	28.695

4. Discussion

Generally, increasing the incident laser energy density will lead to an increase of sintering depth, density and surface roughness. The experimental results from the porosity map in Fig. 5 suggest that laser sintering at laser powers below 20 W produces a porous sintered surface due to low incident laser energy density. Although the porosity in the sintered surface increases with increasing scan rate. The size of the pores and the agglomerates remains small. Likewise, a high heat input from laser powers ranging from 25 to 40 W results in a change of pore morphology from an open (or interconnected) to a closed structure, depending on

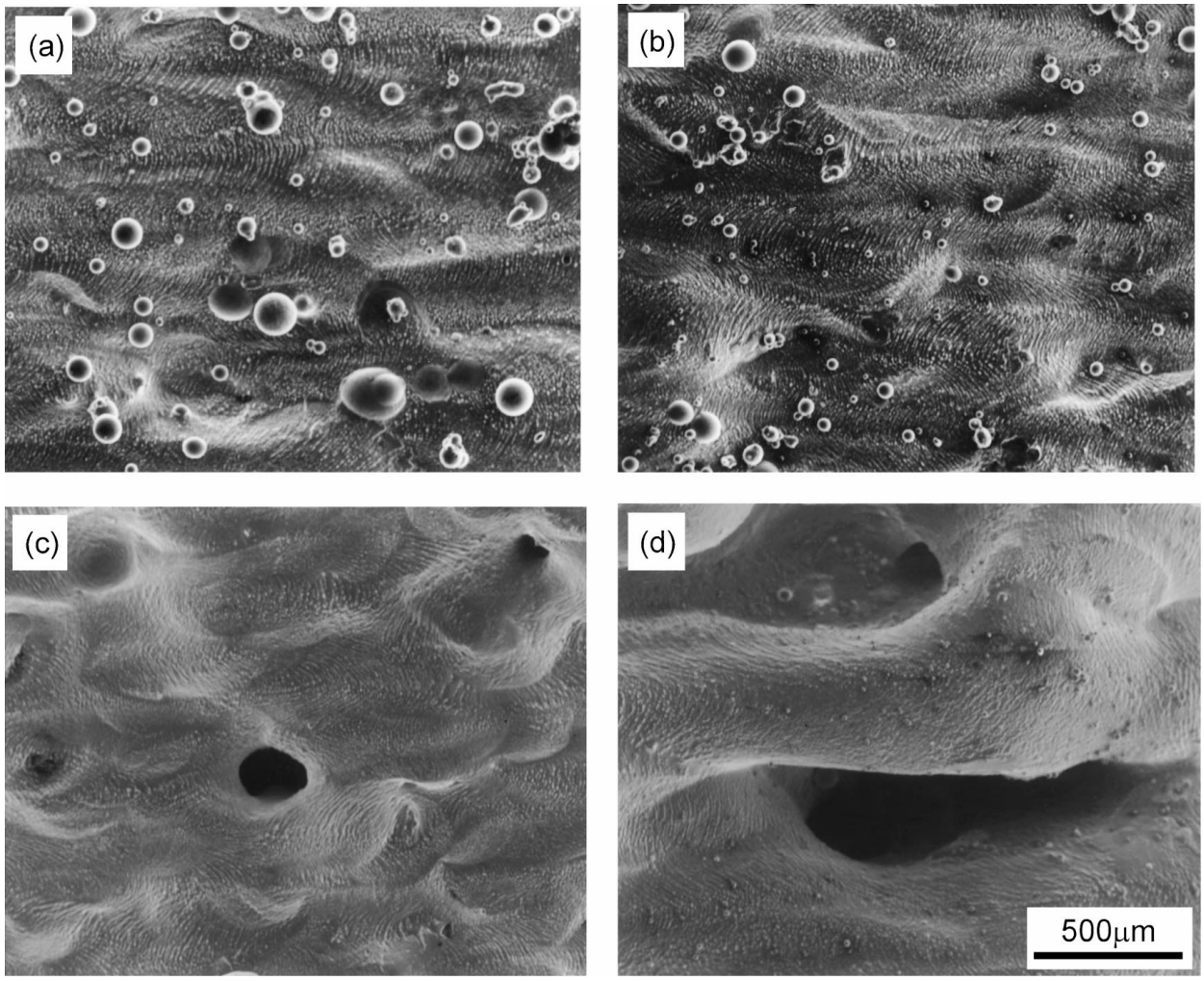

Figure 9 SEM images of laser sintered M2 surfaces using laser powers of 50 W, a scan rate of 5.0 mm/s and a scan line spacing of 0.15 mm: (a) as-supplied; (b) 53–150 μm; (c) >150 μm; (d) <38 μm (Scan direction ↔).

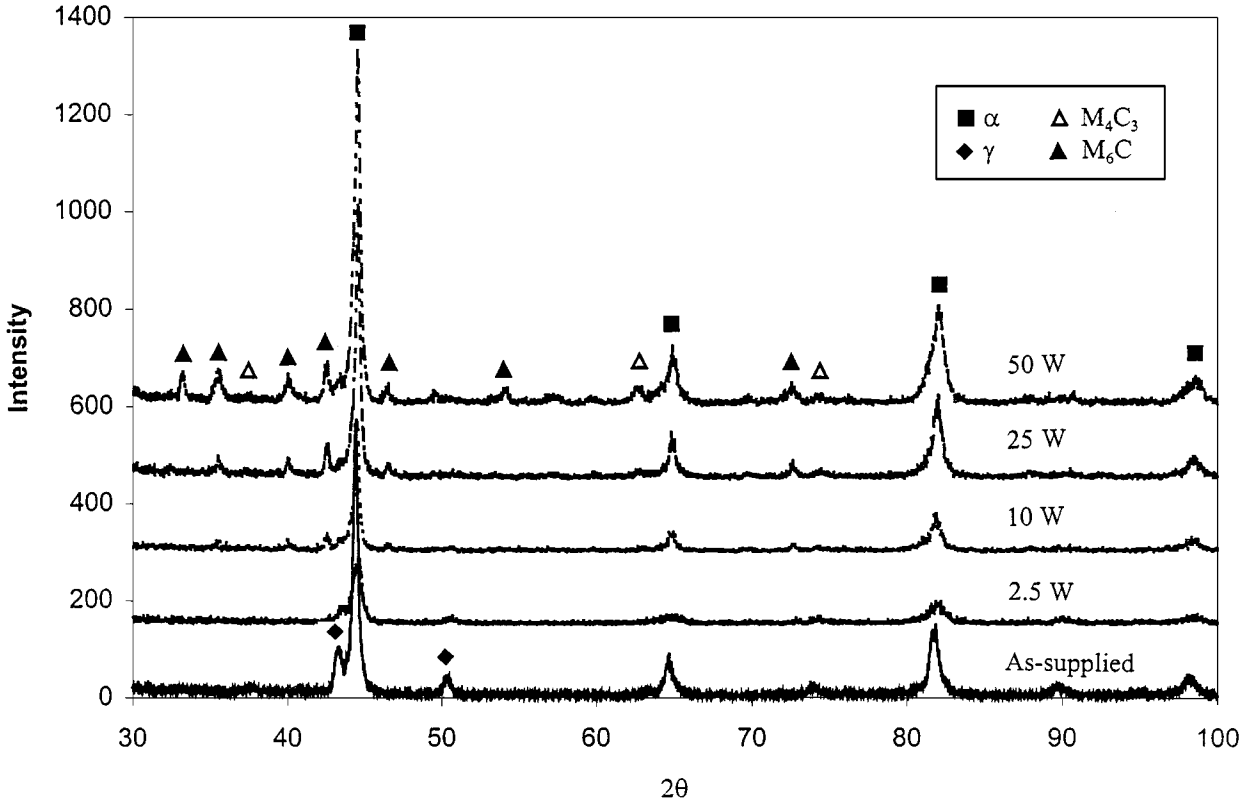

Figure 10 X-ray pattern of the laser sintered samples at different laser powers and a scan rate of 1.0 mm/s.

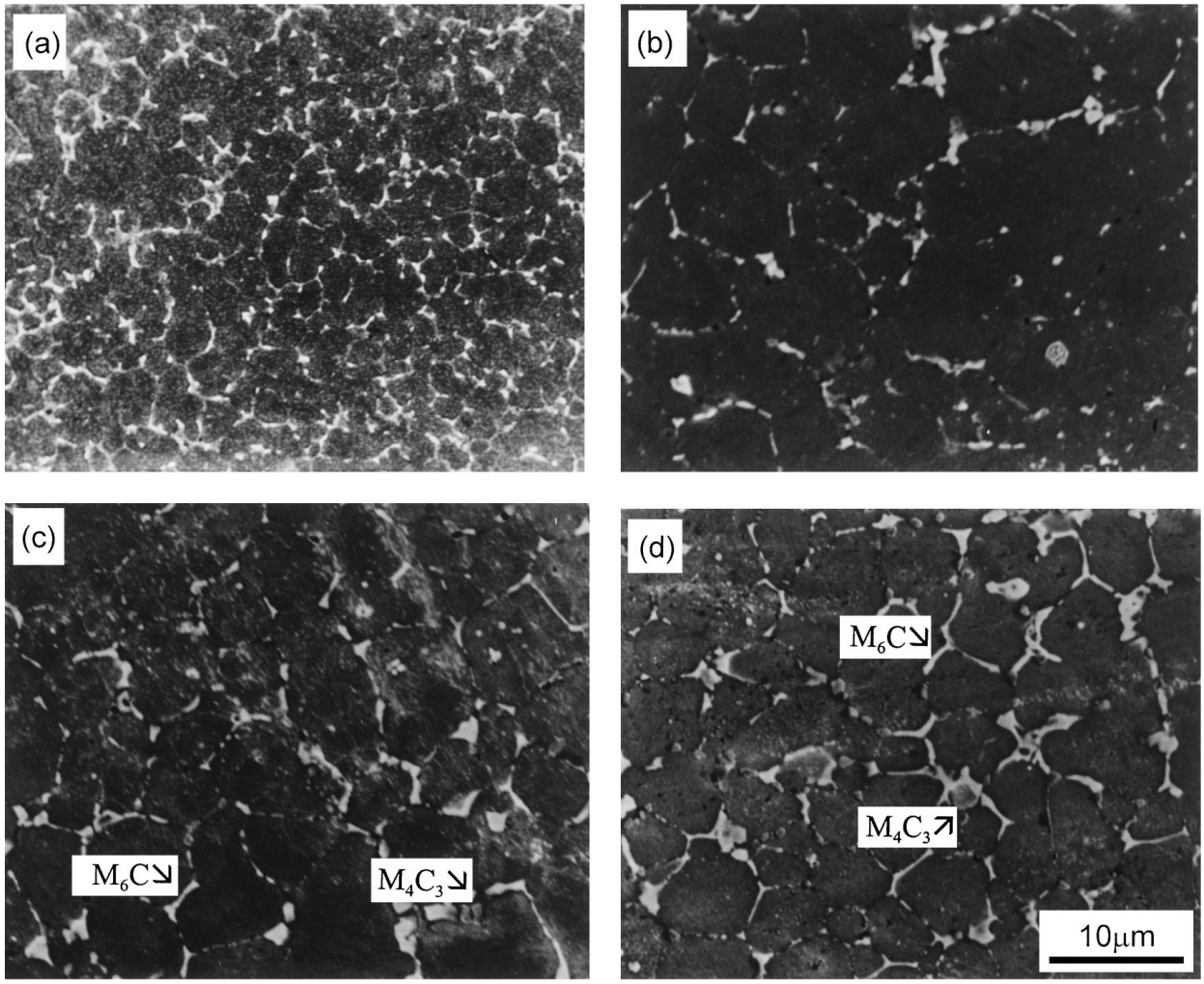

Figure 11 SEM images of the as-supplied M2 powers and the laser sintered M2 HSS samples at different laser powers for a scan rate of 1.0 mm/s: (a) as-supplied; (b) 10 W; (c) 25 W; (d) 50 W.

the scan rate. However, at this stage the surface density increases with increasing scan rate. This abnormal phenomenon may be caused by the competition between coarsening and densification [9]. The SLS at a low scan rate tends to cause the formation of the coarse and dense agglomerates because of the highly localized heat input and greater heat affected zone around the laser beam, thereby increasing agglomeration of powder particles outside the laser beam. While a high scan rate gives a relatively low heat input and smaller heat affected zone, thereby giving less agglomeration outside the laser beam, i.e. densifying first, with relatively small agglomerates and pores. Therefore, when the laser power is higher than a certain value, higher scan rate tends to produce highly dense surface as the smaller pores are easier to be filled. However, on laser sintering at laser powers above 40 W with a low scan rate, the incident energy density is high enough to produce a fully dense surface.

The width of the sintered region per scan decrease with increasing scan rate. For a given length of a scan track, the length/diameter ratio of the track is increased with increasing laser scan rate. This tends to enhance the breakup of liquid metal cylinder caused by Rayleigh instability [5], and thus causes the formation of the lateral pores in the sintered surface.

From Equation 1, the effect of increasing scan line spacing on incident laser energy density is identical to that of decreasing laser power, or increasing scan rate. However, SEM observation suggests that scan line spacing plays an important role on the surface roughness. An excessive overlapping of the scan track (i.e. small scan line spacing) increases the surface roughness due to increasing disturbance of the latter scan on the previous scan (Fig. 7). However, excessively large scan line spacing tends to decrease the binding between the scan tracks and increase the formation of the lateral pore on the sintered surface (Fig. 8).

Fine powder particles have a high surface energy and enhance the laser-powder interaction, leading to an increased sintering reaction [1,10]. Therefore, large powder particles require higher incident laser energy density to obtain a highly dense surface. However, no fully dense surface can be obtained by laser sintering of the fine particles (<38 μm) at laser powers between 5 and 50 W for scan rates between 1 and 30 mm/s. Furthermore, laser sintering of fine powder at a high laser power tends to form the longitudinal pores in the sintered surface. This result may be attributed to a high level of oxygen (375 ppm) present in the fine particles, as compared with that in the as supplied powder particles (200 ppm) and the coarse powder particles (130 ppm). The oxygen

content may be due to either surface oxide layer or to oxygen dissolved in the powder. When the laser power is sufficient to melt the powder particles completely and a melt pool is developed. The motion in this melt pool is driven by the thermocapillary force that causes a fluid flow known as Marangoni flow. The width/depth ratio of the laser scan track is controlled by the direction and magnitude of the thermocapillary force [3,4]. The direction and magnitude of the thermocapillary force is influenced by the surface active elements, such as oxygen. For a example, a high oxygen content tends to result in a decrease of the width/depth ratio [4]. This is likely to cause separation between the tracks, leading to the formation of the longitudinal pores.

5. Conclusions

1. The surface density of laser sintered gas atomized M2 HSS increases with increasing laser power. When laser power is higher than 40 W, a fully dense surface can be obtained.

2. For a range of laser powers between 40 to 80 W and a scan line spacing of 0.15 mm, the laser scan rates required for the production of dense surface ranges from 1 to 25 mm/s according to Fig. 5.

3. Appropriate selection of scan line spacing is important to improve surface density and roughness.

4. Appropriate particle size range is required for the production of smooth dense surface by laser sintering process of M2 powder. Fine M2 powder (<38 μm) tends to give less dense structure after laser sintering due to the presence of high oxygen level.

5. Selective laser sintering of M2 HSS powder results in the formation of the fine grains. The as sintered microstructure consists of ferritic matrix with grain boundary carbides of M_6C, and M_4C_3.

Acknowledgements

The authors would like to thank Powdrex Ltd., UK, for the provision of the powders. In addition, we would like to thank Professor I. R. Harris for the provision of laboratory facilities and ORS awards for the financial support. Finally we would like to thank A. Rogers for the oxygen analysis of the powder.

References

1. A. MANTHIRAM, D. L. BOURELL and H. L. MARCUS, **JOM**, **45** (1993) 66.
2. T. FUESTING, L. BROWN, S. DAS, N. HARLAN, G. LEE, J. J. BEAMAN, D. L. BOURELL, J. W. BARLOW and K. SARGENT, in "Solid Freeform Fabrication Proceedings," Austin, August 1996, edited by D. L. Bourell, J. J. Beaman, H. L. Marcus, R. H. Crawford and J. W. Barlow (The University of Texas at Austin, 1996), p. 39.
3. K. C. MILLS and B. J. KEENE, *Inter. Mater. Rev.* **35** 1990 (185).
4. K. C. MILLS, B. J. KEENE, R. F. BROOKS and A. SHIRALI, *Phil. Trans. R. Soc. Lond. A* **356** (1998) 911.
5. H. NIU and I. T. H. CHANG, *Scripta Materialia* **1** (1998) 67.
6. F. A. KIRK, *Powder Metall.* **24** (1981) 70.
7. J. D. BOLTON and A. J. GANT, *ibid.* **40** (1997) 143.
8. H. NIU and I. T. H. CHANG, *Scripta Materialia* **41** (1999) 25.
9. N. J. SHAW, *Powder Metallurgy International* **21** (1989) 16.
10. D. DOBRANICH and R. C. DYKHUIZEN, Private Communication, Sandia National Laboratories, February 10, 1998.

Received 1 February
and accepted 23 June 1999